

HYBRID COMPUTATION OF NORMAL MODE TUNE SHIFTS IN ROUNDED-RECTANGULAR PIPES*

V. Galdi, D.I.I.E. - Univ. of Salerno, I-84084 Fisciano (SA), Italy
S. Petracca^{†‡}, and I. M. Pinto, Univ. of Sannio at Benevento, I-82100 Benevento, Italy

Abstract

A fast and accurate hybrid (analytical-numerical) technique for computing the normal mode tune-shifts in rounded-rectangular (stadium) pipes is introduced based on Galerkin method together with a smart representation of Poisson's equation Green's function in a rectangular domain. Comparison with standard finite-elements and finite difference methods shows that our method is faster and more accurate, requiring no numerical differentiation.

1 THE PROBLEM

Many beam-pipe cross-section geometries of potential interest for accelerators, including the stadium-shaped one recently proposed for LHC [3], differ from the rectangle only by the rounding of corners, or the substitution of straight sides with circular arcs. Computing the related betatron tune-shifts, resulting from collective (space-charge and image) effects is a key problem to prevent resonant betatron excitations leading to potentially harmful beam instabilities. The normal mode coherent and incoherent¹ tune-shifts can be written in terms of the normal mode Laslett coefficients ϵ as follows [2]:

$$\Delta\nu = -\frac{NRr_0}{\pi\nu\beta_0^2\gamma_0 L^2} \epsilon, \quad (1)$$

where²:

$$\begin{aligned} \epsilon_{1,2} = & \frac{L^2}{4\Lambda} \left\{ -\frac{\delta_x \partial_x \Phi^{(im)} + \delta_y \partial_y \Phi^{(im)}}{2} + \right. \\ & \pm \left[\left(\frac{\delta_y \partial_y \Phi^{(im)} - \delta_x \partial_x \Phi^{(im)}}{2} \right)^2 + \right. \\ & \left. \left. + \delta_x \partial_x \Phi^{(im)} \delta_y \partial_y \Phi^{(im)} \right]^{1/2} \right\}, \quad (2) \end{aligned}$$

$\Phi^{(im)}$ is the image-potential produced in the beam pipe by a linear charge density Λ going through the beam center of charge \underline{r}_b , N is the number of particles in the beam, R is

* Work supported in part by INFN.

† On leave of absence from KEK, Tsukuba, JPN.

‡ e-mail stefania@kek.vax.ac.jp

¹The *incoherent* and *coherent* regimes correspond to $\underline{r} \neq \underline{r}_b = \underline{r}_{eq}$ and $\underline{r} = \underline{r}_b \neq \underline{r}_{eq}$, respectively, \underline{r}_{eq} denoting the beam center of charge equilibrium position [2].

²The pipe-shape independent space-charge contribution to the tune-shift is neglected here for simplicity.

the machine radius, r_0 is the classical particle radius, L is a scaling length (usually, the maximum pipe diameter), ν is the nominal tune, and

$$\left\{ \begin{array}{l} \delta_{x,y} = \partial_{x,y}|_{\underline{r}=\underline{r}_b}, \text{incoherent regime,} \\ \delta_{x,y} = (\partial_{x,y} + \partial_{x_b,y_b})|_{\underline{r}=\underline{r}_b}, \text{coherent regime.} \end{array} \right. \quad (3)$$

2 THE METHOD

For computing the image potential $\Phi^{(im)}$ in rounded rectangular geometries, it is convenient to use the rectangular-domain Green's function g_R (henceforth RDGF), viz. :

$$\begin{aligned} \Phi^{(im)}(\underline{r}, \underline{r}_b) &= \Phi(\underline{r}, \underline{r}_b) - \Lambda g_0(\underline{r}, \underline{r}_b), \\ \Phi(\underline{r}, \underline{r}_b) &= \Lambda \left[\sum_k \int_{\sigma_k} g_R(\underline{r}, l_k) \rho_{\sigma_k}(l_k) dl_k + g_R(\underline{r}, \underline{r}_b) \right], \quad (4) \end{aligned}$$

where g_0 is the free-space Green's function, the unknown ρ_{σ_k} are obviously nonzero *only* on the rounded portion of ∂S_0 , i.e., the arcs σ_k , and l_k is the arc-length on σ_k .

We seek a hybrid (analytical-numerical) solution of eq. (4) by using Galerkin (moments) method [6], whereby we first expand the unknown ρ_s :

$$\rho_{\sigma_k}(l_k) = \sum_{n=1}^N b_n^{(k)} w_n^{(k)}(l_k), \quad (5)$$

into a suitable (finite) set of basis functions $\{w_1^{(k)}(l_k), \dots, w_N^{(k)}(l_k)\}$, defined on σ_k , where $\{b_1^{(k)}, \dots, b_N^{(k)}\}$, are N -dimensional vectors of unknown coefficients, and then enforce the (Dirichlet) boundary conditions on the arcs σ_k , whence:

$$\int_{\sigma_k} \Phi(l_k, \underline{r}_b) w_n^{(k)}(l_k) dl_k = 0, \quad n = 1, 2, \dots, N; \quad k = 1, 2, \dots, P, \quad (6)$$

thus obtaining a block-matrix linear system:

$$[\mathbf{L}] \mathbf{b} = \mathbf{c}. \quad (7)$$

The matrix $[\mathbf{L}]$ is readily shown to be symmetrical, positive definite and hence non-singular. The components of \mathbf{b} , \mathbf{c} and \mathbf{L} are explicitly given by (5),

$$c_i^{(k)} = - \int_{\sigma_k} w_i^{(k)}(l_k) g(l_k, \underline{r}_b) dl_k,$$

$$i = 1, 2, \dots, N; \quad k = 1, 2, \dots, P, \quad (8)$$

and:

$$[L_M^{(p,q)}]_{ij} = \int_{\sigma_p} \int_{\sigma_q} g(l_p, l_q) w_i^{(p)}(l_p) w_j^{(q)}(l_q) dl_p dl_q, \\ i, j = 1, 2, \dots, N, \quad p, q = 1, 2, \dots, P, \quad (9)$$

where the upper indexes identify the block sub-matrix, and the lower ones the element in each sub-matrix.

Using eq.s (2)-(5), once (7) has been solved, the Laslett coefficients can be computed *without* resorting to numerical differentiation. This makes the proposed method definitely more accurate than both finite-differences and finite-elements.

3 IMPLEMENTATION AND COMPUTATIONAL BUDGET

Fast and accurate numerical solution of (7) follows from a skillful choice of the RDGF representation in (4) and the basis functions in (5).

A rapidly converging series expansion of the RDGF [5], which explicitly contains the (logarithmic) singular term is ³:

$$g_R(\underline{r}, \underline{r}_b) = - \sum_{m=-\infty}^{\infty} \log \frac{T_m^{10}(\underline{r}, \underline{r}_b) T_m^{01}(\underline{r}, \underline{r}_b)}{T_m^{00}(\underline{r}, \underline{r}_b) T_m^{11}(\underline{r}, \underline{r}_b)}, \quad (10)$$

where:

$$T_m^{pq}(\underline{r}, \underline{r}_b) = 1 + \exp \left[-2 |y - (-)^p y_b + 2bm| \frac{\pi}{a} \right] + \\ -2 \exp \left[|y - (-)^p y_b + 2bm| \frac{\pi}{a} \right] \cos \left[\frac{\pi}{a} (x - (-)^q x_b) \right], \quad (11)$$

a, b being the rectangle side lengths.

A convenient set of (partially overlapping) piece-wise parabolic *subdomain* basis functions, can be defined in terms of the local angles ϕ (we drop the suffix k for simplicity) as follows:

$$w_i(\phi) = \frac{\Delta\phi^2 - (\phi - \phi_i)^2}{\Delta\phi^2}, \\ \phi_i - \Delta\phi(1 - \delta_{i1}) \leq \phi < \phi_i + \Delta\phi(1 - \delta_{iN}), \\ i = 1, 2, \dots, N, \quad (12)$$

where $\Delta\phi$ is the angular discretization step (assumed the same for all arcs), ϕ is related to the local arc-length l by $l = R\phi$, R being the local curvature radius, and δ_{rs} is the Kronecker symbol⁴. The relevant local coordinate systems are sketched in Fig. 1. Note that: *i*) the choice of *subdomain* basis functions, rather than *full-domain* ones, results

³It is easily recognized that the (logarithmic) singularity of g_R appears in the T_0^{10} term.

⁴For $i = 1, N$, eq. (12) yields the correct behaviour at the points where the circular arcs join the straight portions of ∂S_0 , where ρ_s can be different from zero, but its derivative should vanish.

into *fewer* singular integrals in $[\mathbf{L}]$; *ii*) *no* polygonal approximation of the arcs is implied, resulting into fewer functions being needed for a given accuracy.

Letting P the number of arcs in the rounded portion of ∂S_0 , the system (7) has rank NP . Computing the matrix elements requires evaluating up to $PN(PN - 1)/2$ double-integrals⁵. These latter can be either evaluated numerically using standard routines appropriate for regular [7] and singular integrands [8], or analytically [4]. Matrix inversion for solving (7) is not the most demanding task, in view of the typically small ($NP \approx 20$) \mathbf{L} matrix size. In all numerical simulations below we truncated (10) at $|m| \leq 3$ and took $\Delta\phi = \pi/10$, corresponding to a matrix size $NP = 20$.

4 NUMERICAL RESULTS AND CONCLUSIONS

The circular pipe, for which the tune-shifts are known exactly, is the hardest conceivable test case for the proposed method (largest departure from rectangular geometry). It is seen from Fig. 2 that the obtained accuracy is very good.

Our method was subsequently applied [4] to a number of different proposed geometries relevant to LHC [3].

As an example the contour-level plots for the incoherent and coherent (both normal modes) Laslett coefficients for a stadium-shaped pipe, sketched in Fig. 3, are shown in Fig.s 4-6.

As a conclusion, we found that the above hybrid approach is comparatively faster and more accurate than available finite-element and/or finite-difference techniques.

5 REFERENCES

- [1] L.J. Laslett, Proc. of the 1963 Summer Study BNL 7534.
- [2] S. Petracca, Particle Accel., **48**, 81, 1994.
- [3] The LHC study group, CERN/AC/95-05 (LHC), 1995.
- [4] V. Galdi, S. Petracca, I. Pinto, Particle Accel., PA(R)-85, 1999, in print.
- [5] M. Bressan and G. Conciauro, Alta Frequenza, **LII**, 188, 1983, *ibidem* **LVII**, 217, 1988.
- [6] R.F. Harrington, *Field Computation by Moment Methods*, McMillan, New York, 1961.
- [7] W.H. Press et al., *Numerical Recipes, the Art of Scientific Computing*, 2nd Ed., Cambridge Un. Press, 1992.
- [8] SLATEC Pub. Dom. Math. Lib., NETLIB, <http://www.netlib.org>

⁵Due to geometrical (specular) symmetries, the effective number of elements to compute is usually smaller.

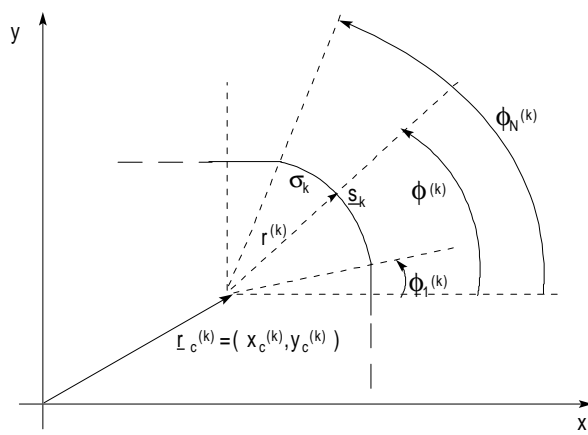


Fig. 1 - Local coordinate system relevant to eq. (12).

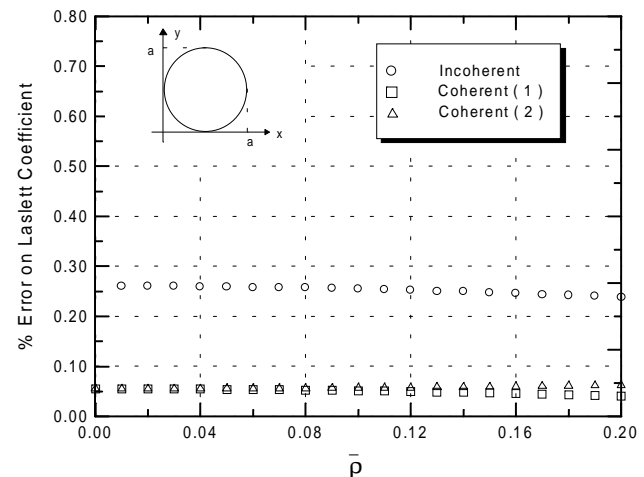


Fig. 2 - Circular pipe. Errors on Laslett coefficients vs. scaled radial distance, $\bar{\rho} = \frac{2}{a} \left[(x - a/2)^2 + (y - a/2)^2 \right]^{1/2}$.

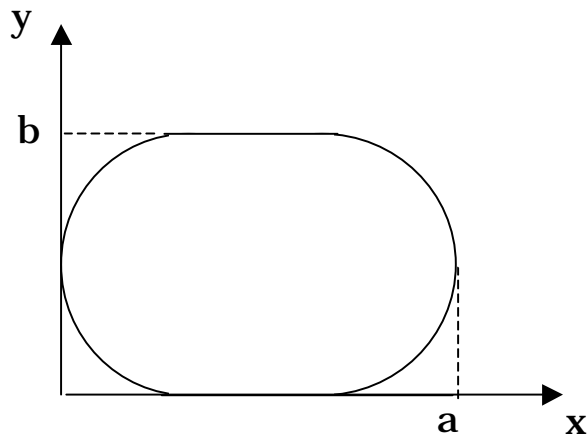


Fig. 3 - Stadium-shaped pipe ($a=1$, $b=0.7$).

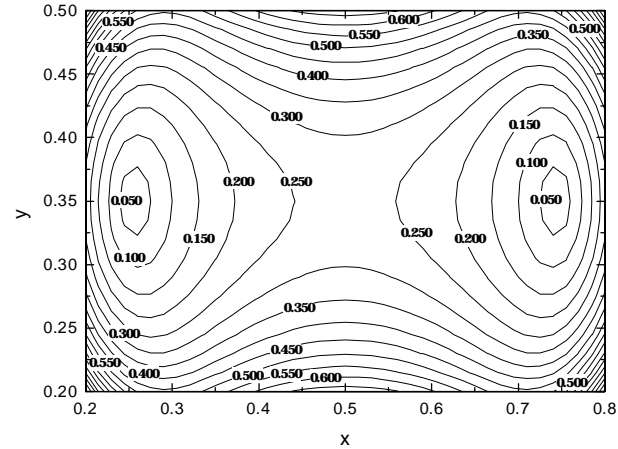


Fig. 4 - Stadium-shaped pipe. Incoherent Laslett coefficients (both normal modes).

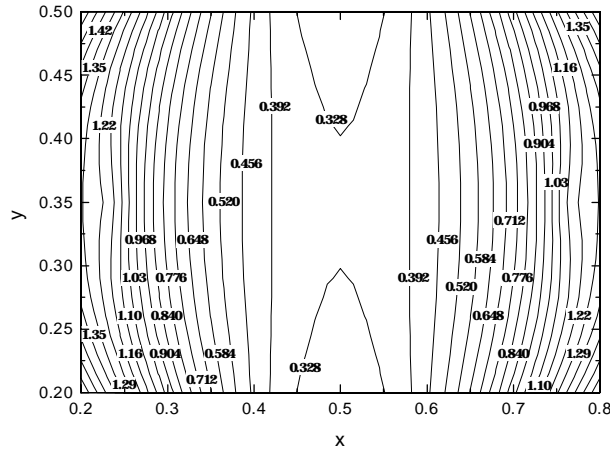


Fig. 5 - Stadium-shaped pipe. Coherent Laslett coefficient (1st normal mode).

